Title: Pleiotropy drives repeatability in the genetic basis of adaptation

Short running title: Pleiotropy drives repeatability in adaptation

Authors: Paul Battlay[1], Sam Yeaman[2], Kathryn A. Hodgins[1]

1. School of Biological Sciences, Monash University, Melbourne, Victoria, Australia

2. Department of Biological Sciences, University of Calgary, Calgary, Alberta, Canada

Corresponding author: Paul Battlay; pbattlay@gmail.com

Author contributions: Paul Battlay: Data curation, Formal analysis, Investigation, Software, Visualization, Writing - original draft, Writing - review & editing **Sam Yeaman:** Conceptualization, Methodology, Supervision, Writing - review & editing **Kathryn A. Hodgins:** Conceptualization, Funding acquisition, Methodology, Project administration, Supervision, Writing - review & editing

Acknowledgements: We thank Tim Connallon and Jacqueline Sztepanacz for valuable feedback on the manuscript. Funding was provided by a Human Frontier Science Program grant to KAH.

Data Accessibility Statement: Simulation Eidos scripts and analysis R code is available at https://github.com/pbattlay/pleio-sims/

Pleiotropy drives repeatability in the genetic basis of adaptation

Paul Battlay[1], Sam Yeaman[2], Kathryn A. Hodgins[1]

1. School of Biological Sciences, Monash University, Melbourne, Victoria, Australia

2. Department of Biological Sciences, University of Calgary, Calgary, Alberta, Canada

Abstract

Studies of trait-mapping and local adaptation often identify signatures of genetically parallel evolution, where different species evolve similar phenotypes using the same genes. Such patterns appear incongruent with current estimations of quantitative trait architecture. With hundreds or thousands or genes contributing to a trait, why would selection make repeated use of the same genes? Here, we use individual-based simulations to explore a two-patch model with quantitative traits and pleiotropy to understand the parameters which may lead to repeated use of a particular locus during independent bouts of adaptation. We find that repeatability can be driven by increased phenotypic effect size, a reduction in trait dimensionality and a reduction in mutational correlations at a particular locus relative to other loci in the genome, and that these patterns are magnified by increased migration between demes. These results suggest that evolutionary convergence can arise from multiple characteristics of a locus, and provide a framework for the interpretation of quantitative signatures of convergence in empirical studies.

Keywords: pleiotropy, parallel evolution, repeatability, migration, simulations

Introduction

Studies of adaptation commonly observe convergent genetic responses, where multiple species independently respond to a given selection pressure with mutations in orthologous genes [1–4]. These patterns imply a lack of redundancy in the genes available for a selective response [5,6], and at first glance seem inconsistent with another common observation: that variation in quantitative traits is explained by a very large number of alleles of small effect [7,8], which suggests a high level of redundancy in the genes contributing to quantitative traits.

In the early 20th century, theoretical work by R. A. Fisher demonstrated that the continuous phenotypic variation observed in populations could be explained by a large number of alleles inherited in a Mendelian manner [7], and that selection would favor small-effect changes at large numbers of loci [9]. Genome-wide association studies in humans have provided empirical observations of standing variation congruent to Fisher's models of adaptive trait architecture (reviewed in [10]): Associations with hundreds or thousands of genetic variants explain only a modest proportion of trait heritability, with the remaining heritability attributable to even larger numbers of variants with effect sizes too small to detect with current cohorts (or possibly to rare variants that are excluded from many such analyses). But if variation in thousands of genes underpins a given trait, why would we ever observe orthologous genes contributing to adaptation in multiple species, when there are seemingly a myriad of ways to construct the same traits?

In his revisiting of Fisher's model, Kimura [11] demonstrated that although smaller effect mutations are more likely to be favourable, beneficial mutations of small effect are less likely to fix, as genetic drift biases the contribution of intermediate-effect loci to adaptation. Later, Orr [12] showed that effect sizes of fixed adaptive mutations during an adaptive walk should be exponential, illustrating the importance of large-effect mutations early in bouts of adaptation to a new and distant environmental optimum. The omnigenic model (which posits that all genetic variants in genes expressed in the relevant cell type contribute to a phenotype; [8,13]) also makes the distinction between 'core' genes of larger effect and 'peripheral' genes of small effect (although the latter explains the bulk of trait heritability). Perhaps the simplest explanation for convergent genetic adaptation is if alleles of large effect are disproportionately likely to contribute to adaptation (e.g., because of their fixation probabilities), but only a subset of loci are able to generate alleles of large effect [14]. Convergence in gene use would then occur if there is long-term conservation of the genotype-phenotype map and the potential for particular loci to

77 generate alleles of large effect. Certainly, large-effect QTL have been identified in both
78 experimental evolution studies (e.g. [15]) and natural populations (e.g. [16,17]), and genomic
79 footprints of selective sweeps [18,19] provide evidence for strong selection at individual loci
80 [20,21]. The effects of local adaptation on genetic architecture may further act to increase the
81 likelihood of repeatability, as the contributions of small-effect alleles are disproportionately
82 limited by the swamping effect of gene flow in populations connected by migration [22].
83 Consequently, convergence in the genetic basis of local adaptation is expected to frequently
84 involve large-effect mutations, particularly when gene flow is high or drift is strong, yet these
85 processes do not overwhelm selection [6].
86
87 While alleles of large effect may be favoured early in adaptation or when there is migration-
88 selection balance, their contribution to adaptation can be limited by pleiotropy. In both Fisher's
89 [9] and Orr's [12] models, mutations are modelled as vectors in multidimensional phenotypic
90 space; therefore mutations with a large effect in a favorable dimension generally deviate too far
91 from the optima in other dimensions, with serious fitness consequences (e.g. [23]). Chevin,
92 Martin & Lenormand [24] expanded these models to incorporate distinct genes which could vary
93 in their pleiotropic properties: specifically the number of traits that mutations would affect, and
94 the correlation in effects of mutations on different traits (the latter being a property that can arise
95 from organization of genes into networks; [25]). They demonstrated that repeatability in the
96 genetics of adaptation is an expected consequence of between-locus variation in pleiotropy;
97 convergence may therefore be observed in genes where negative fitness effects of pleiotropy
98 are minimized.
99
100 Previous models provide expectations for the contribution of pleiotropy and effect size to
101 repeatability in isolated populations, however the interaction of these parameters with gene flow
102 in locally-adapting populations has not been studied. This stands in contrast to the growing body
103 of empirical work describing repeatability in locally-adapting populations and divergent lineages
104 with gene flow [1–4]. To provide a theoretical grounding for such studies, we utilize individual-
105 based simulations of quantitative trait evolution examining how the interplay between inter-locus
106 heterogeneity in pleiotropy and migration-selection balance affects genetic convergence. We
107 build on previous models, which have considered adaptation in a single population following an
108 environmental shift, by introducing a second population adapting to a divergent environment,
109 allowing the observation of interactions between migration, effect size and pleiotropy in bouts of
110 local adaptation. We find that increasing effect size or decreasing pleiotropy (both the overall

111 dimensionality as well as mutational correlation) at a given QTL relative to the other QTL will
112 increase repeatability. Moreover we find that increased migration between demes exacerbates
113 the repeatability observed.

Simulations

To study the factors driving repeatability at particular loci in independent bouts of adaptation, we performed Wright-Fisher, forward-time simulations in SLiM (v. 3.3.1; [26]) with adaptation to a complex environment that varied across two patches connected by migration. Adaptation within each patch was driven by selection on two (or more) traits: Z_1 with an optimum that varied among the patches, and one or more (e.g. Z_2) with the same optimum in each patch.

To gain insight into the parameters capable of driving repeatability at a particular locus and their interaction, we simulated a simplified genome: Traits could be affected by mutations at five genetically unlinked QTL; recombination within QTL occurred at a rate of 2.5×10^{-7}. Properties were uniform across four QTL, while aberrant properties were assigned to a single 'focal 'QTL, where parameter values could be varied independently of the non-focal QTL. For some parameters, simulations were repeated with a total of 20 QTL and one focal QTL (fig. S3). Each QTL consisted of 500bp, and mutations occurred at a rate of 1×10^{-7} per base pair per generation, resulting in an expected 10,000 mutations in each of two demes over the 20,000-generation simulation.

QTL mutations affected two or more phenotypes (e.g. Z_1 and Z_2); mutational effects for each QTL were drawn from a multivariate normal distribution with variance a^2, which determines the QTL effect magnitude, and covariance which was equal to the QTL mutational correlation multiplied by a^2.

The following Gaussian function related individual fitness to phenotype Z_i:

$$w_i = e^{-\frac{(\theta_i - \Sigma a_i)^2}{2V_s}} \quad (1)$$

where θ_i = the phenotypic optimum and Σa_i = the sum of mutation effects for phenotype Z_i, and V_s = the variance in the fitness function, reflecting the strength of stabilizing selection (set at 125 for all simulations). Overall individual fitness was calculated as the product of w across all phenotypes, so there was no correlational selection between pairs of phenotypes.

We simulated two demes (d_1 and d_2), each composed of 1000 randomly-mating diploid hermaphroditic individuals. Phenotypic space was unitless and provided a relative scaling for

the width of the fitness function and the magnitude of mutational effects. Both demes began the simulation with phenotypic optima of 0 for all phenotypes and ran with a burn-in for 20,000 generations. After the burn-in, phenotypic optima were shifted and we tracked adaptive evolution over the following 20,000 generations. For most simulations, we focussed on the case where in d_1 the optima for all phenotypes remained at 0, while in d_2, the optimum for Z_1 was shifted to -10, while Z_2 (and optima for any other phenotypes) remained at 0. We varied the migration rate between d_1 and d_2 (from 0 to 0.05) and α^2 (from 0.1 to 5), mutational correlations (from 0 to 0.99), and the number of phenotypes affected by the QTL.

We investigated three main ways in which the characteristics of the focal QTL could be differentiated from those of the other loci:

1) A change in α^2 by altering the variance component of the variance-covariance matrix used to generate mutations (fig. 1A cf. B). This parameter was used to model a large-effect QTL at the focal QTL.
2) A change in mutational correlation by altering the covariance component of the variance-covariance matrix (fig 1A cf. C). This parameter models dependence between phenotypes and determines the likelihood that a mutation's effect on one phenotype will have a corresponding effect on another.
3) A change in the number of phenotypes affected by a mutation by reducing the dimensionality of the variance-covariance matrix (fig. 1A cf. D). This models a situation where a QTL has no effect on one or more phenotypes..

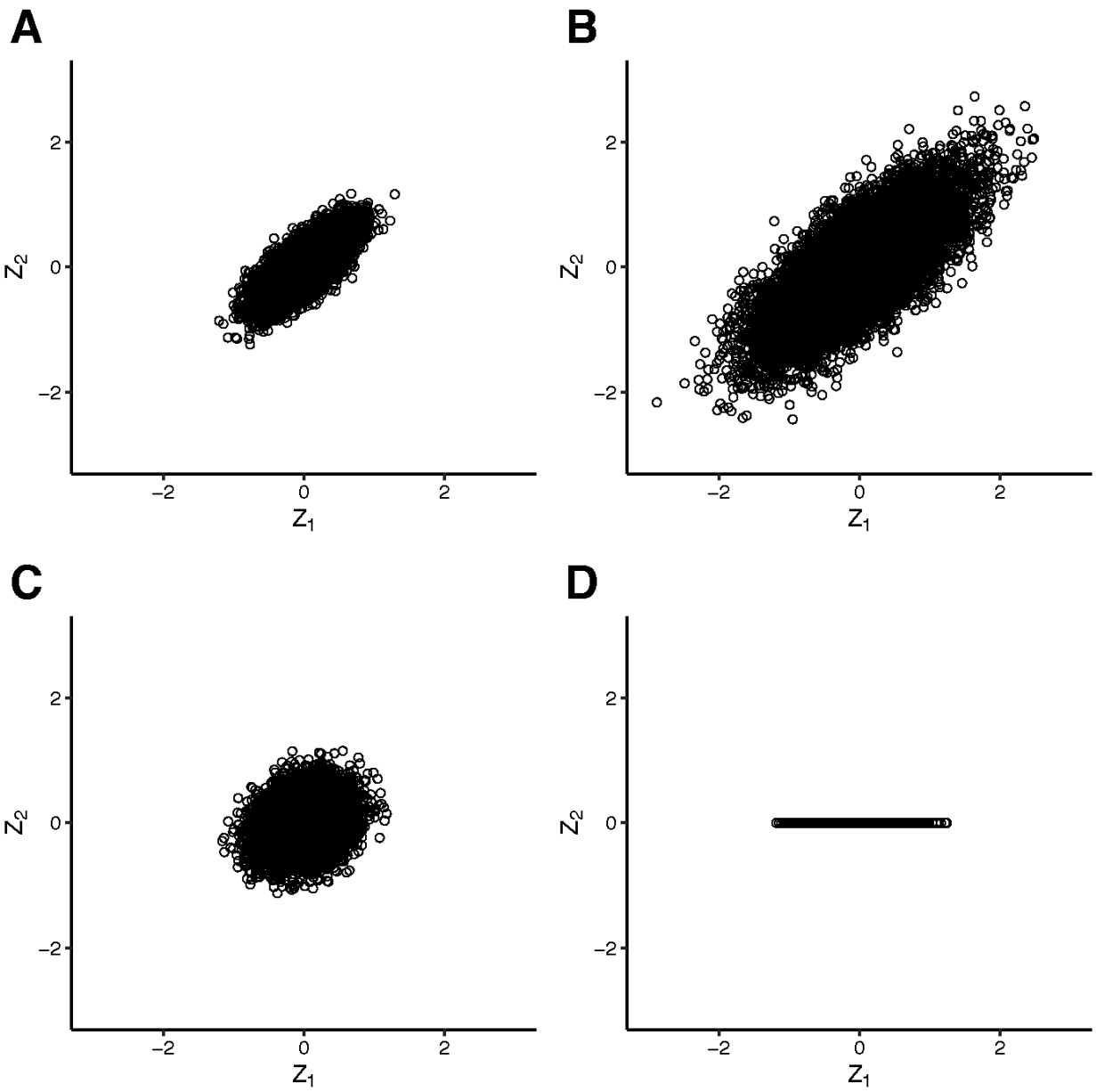

Figure 1. Effect sizes on Z_1 (x-axes) and Z_2 (y-axes) for 10,000 draws from distributions used to generate mutations. In A, a^2 is 0.1 and the mutational correlation between traits is 0.75. In B, the mutational correlation is the same as A (0.75) but a^2 is increased to 0.5. In C, a^2 is the same as A (0.1), but the mutational correlation is relaxed to 0.25. In D, mutations have no effect on the non-divergent phenotype.

To interpret the results of each parameter combination, we calculated the genetic value (*GV*) that a given genomic region (e.g., a QTL) contributes to phenotypic divergence using the formula:

$$GV = \sum((p_1 - p_2) \times a) \quad (2)$$

where p_1 and p_2 are the frequencies of a mutation in each deme, and a is the size of the mutation's effect on Z_1.

For each parameter combination we quantified the divergence (the difference in mean phenotypes) between demes d_1 and d_2 at the divergently selected phenotype with $2\times GV_{all}$ (*GV* summed across all QTL), and quantified repeatability in the contributions of the QTL to trait divergence (measured by QTL-specific *GV*) across 100 replicates using the C_{chisq} statistic with 1000 permutations [6], implemented in the dgconstraint R package [6] with the *pairwise_c_chisq()* function (i.e., each replicate is treated as an independent bout of evolution). Briefly, χ^2 was calculated across simulation replicates with:

$$\chi^2 = \frac{\Sigma(G\bar{V}_n - G\bar{\bar{V}}_n)^2}{G\bar{\bar{V}}_n} \quad (3)$$

where $G\bar{V}_n$ is the sum across simulation replicates of *GV* for the n^{th} QTL, and $G\bar{\bar{V}}_n$ is the mean $G\bar{V}_n$ across all QTL.

The C_{chisq} statistic was then calculated by using $\chi^2$and χ^2_{sim}, the results of 1000 permutations of the data within each replicate:

$$C_{chisq} = \frac{\chi^2 - mean(\chi^2_{sim})}{sd(\chi^2_{sim})} \quad (4)$$

By this equation, when C_{chisq}=0 we observe no more repeatability than would be expected by chance. The maximum value of C_{chisq} varies with the number of QTL modelled: C_{chisq}=2 for five QTL and C_{chisq}≈4.36 for 20 QTL.

200 Additionally, we calculated GV_{focal} / GV_{all}, the proportion of *GV* summed across all QTL
201 explained by *GV* summed across the focal QTL.

Results

We began by examining the behavior of models with different arrangements of phenotypic optima, while increasing α^2 at the focal QTL and holding α^2 constant at non-focal QTL. Divergent optima result in divergent phenotypes (fig. 2B; C), although divergence to a heterogeneous optimum is constrained by high mutational correlations (fig. 2C), as found by Guillaume [27]. QTL have equal probability of contributing to adaptation (C_{chisq}=0) when all loci have the same α^2 and mutational correlation (fig. 2 where focal QTL α^2=0.1), but repeatability was observed with any increase in focal QTL α^2 in models with divergent phenotypes (fig. 2). For the remainder of this study, we focus on the phenotypic arrangement in fig. 2C, where repeatability occurs but divergence is affected by mutational correlations (pleiotropy) between heterogeneous optima.

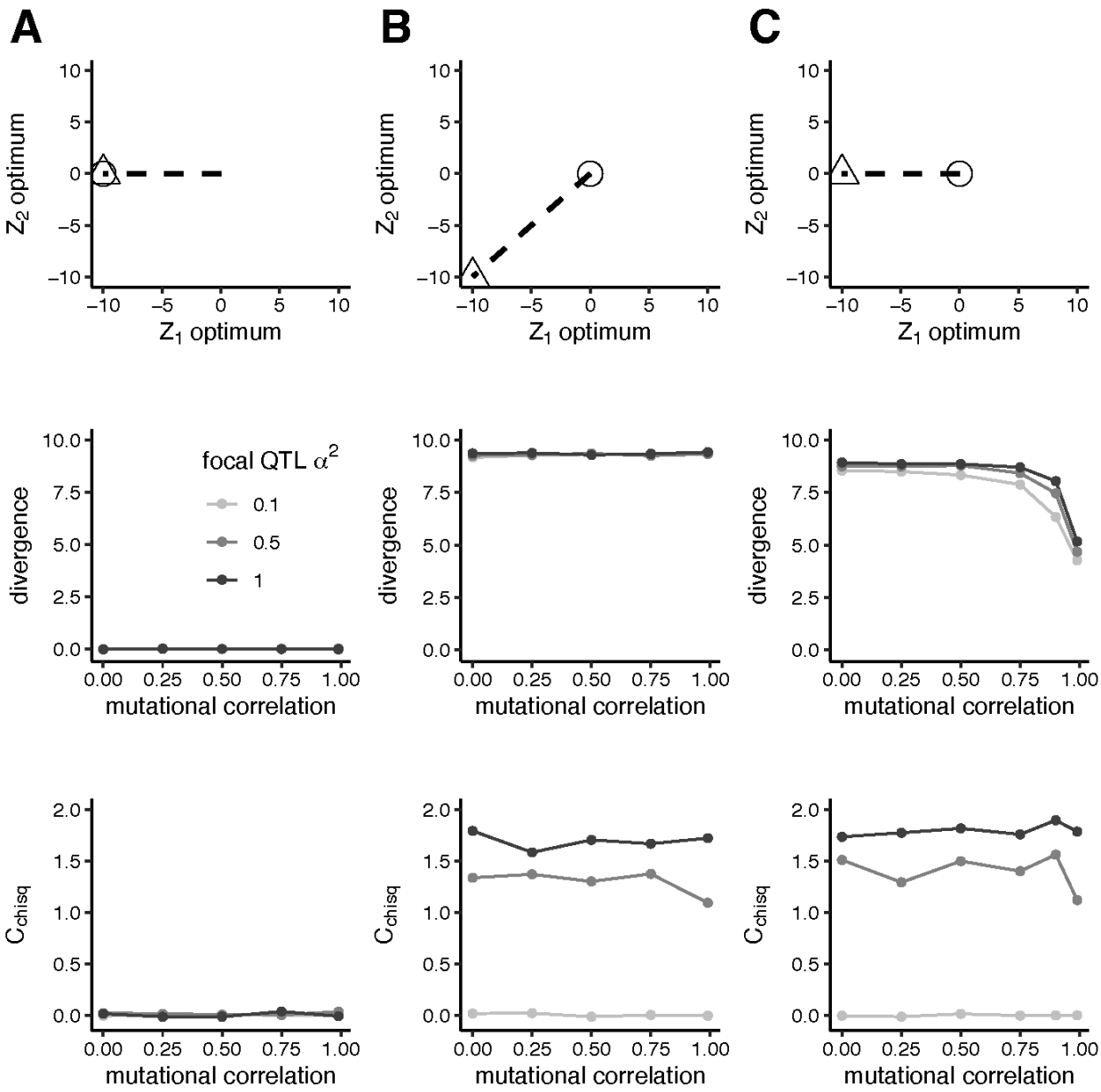

Figure 2. Divergence and repeatability (C_{chisq}) in Z_1 for three arrangements of phenotypic optima: A, where d_1 (circle) and d_2 (triangle) both shift to a heterogeneous environment; B, where d_2 alone shifts to a homogeneous environment; C, where d_2 alone shifts to a heterogeneous environment. α^2 at the focal QTL is varied, while α^2 for non-focal QTL is 0.1. Mutational correlations are uniform at all QTL, and the migration rate is 0.005. These simulations use two phenotypes (one divergent and one non-divergent), and were run for 20,000 generations.

The repeatability observed with increased focal QTL a^2 was robust to variation in migration rate (fig. 3A), and was reflected by an increasing contribution of the focal QTL to divergence (fig. 3C). While high mutational correlations impeded phenotypic divergence, comparable levels of repeatability were observed between high and low mutational correlations unless migration was absent (fig. 3A c.f. B). This is because high mutational correlations limit the rate of, but do not completely exclude the occurrence of mutations with fortuitous combinations of effects (fig. S2A). Furthermore, increasing migration rates resulted in increasing repeatability (fig. 3; fig. S1), and this pattern was exacerbated by increasing mutational correlations.

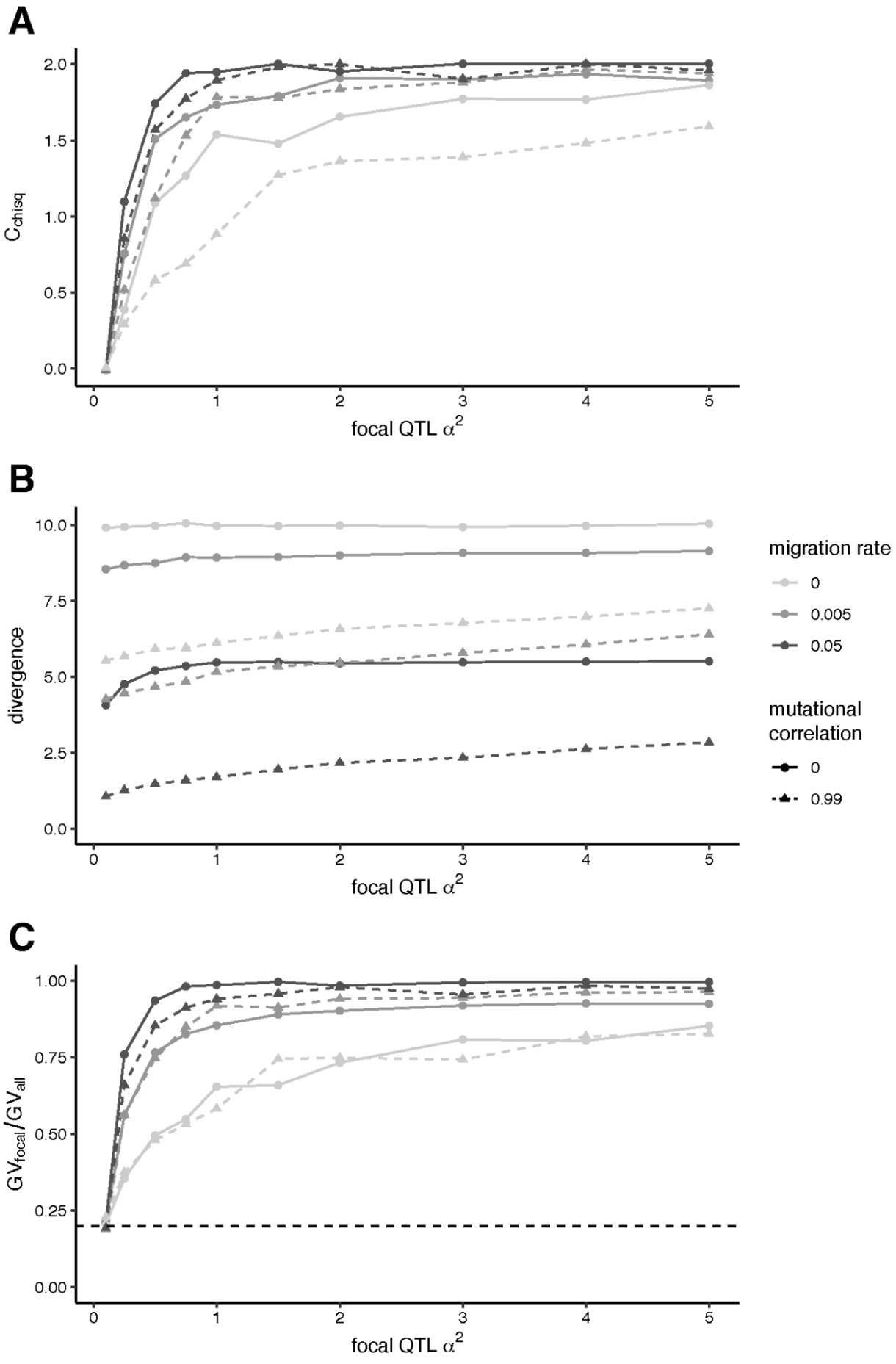

Figure 3. Repeatability (C_{chisq}) in Z_1 (A), Z_1 phenotypic divergence ($2\times GV_{all}$) between d_1 and d_2 (B), and the corresponding mean proportion of all GV explained by GV at the focal QTL (C) against focal QTL a^2 where the a^2 for non-focal QTL is 0.1. The dotted line indicates $GV_{focal} / GV_{all} = 0.2$, the point at which this value shifts from representing overuse of the focal QTL to underuse of the focal QTL. Mutational correlations between phenotypes at all QTL are 0 (circle points; solid lines) or 0.99 (triangle points; dashed lines). These simulations use two phenotypes (one divergent and one non-divergent), and were run for 20,000 generations.

Reducing the correlation in phenotypic effects at a given QTL may also allow it to more readily acquire adaptive mutations when the direction of change toward the optimum is not aligned with the correlation in phenotypic effects (thereby increasing its repeatability). We modeled this by independently varying mutational correlations at the focal and non-focal QTL (fig. 4; fig. S3), and observed repeatability where there were differences between mutational correlation values at focal and non-focal QTL (fig. 4). When the mutational correlation at the focal QTL was reduced relative to the non-focal QTL, repeatability involving the focal QTL increased, and when the mutational correlation at the focal QTL was increased relative to the non-focal QTL, repeatability involving the focal QTL decreased, although this latter observation was not robust to an increase in the number of QTL (fig. S4). High levels of repeatability were only seen when the focal QTL had a relaxed mutational correlation against a background of high mutational correlation at non-focal QTL (i.e. 0.75 and particularly 0.9). This reflects the fact that mutational correlations need to be high to significantly limit the availability of mutations with fortuitous combinations of effects (fig. S2B).

250

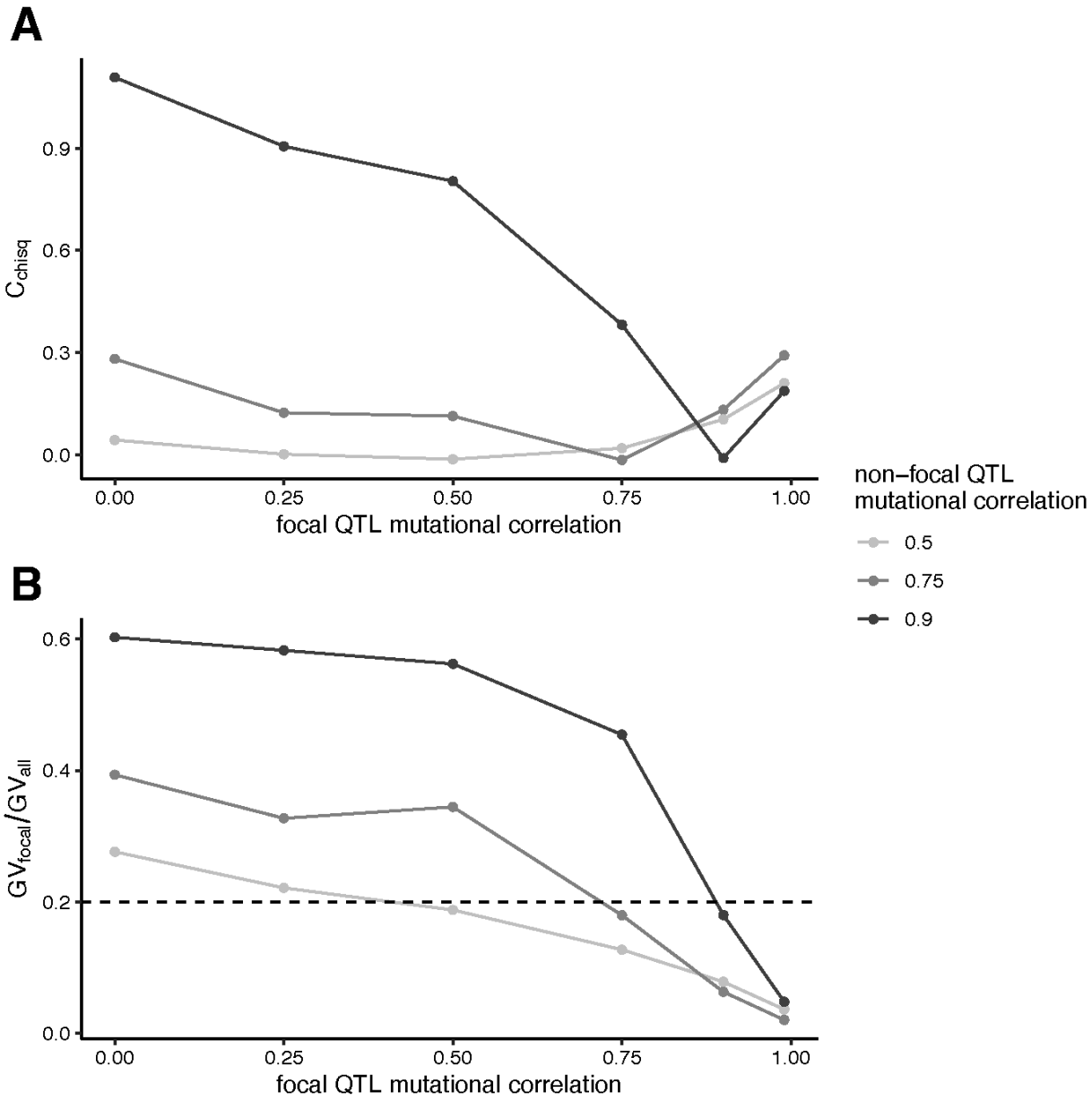

251

252 **Figure 4.** Repeatability (C_{chisq}) in Z_1 against focal QTL mutational correlation for varying values of non-
253 focal QTL mutation correlation (A), and the corresponding mean proportion of all *GV* explained by *GV* at
254 the focal QTL (B). The dotted line indicates $GV_{focal} / GV_{all} = 0.2$, the point at which this value shifts from
255 representing overuse of the focal QTL to underuse of the focal QTL. These simulations use a migration
256 rate of 0.005, an a^2 of 0.5 and two phenotypes (one divergent and one non-divergent), and were run for
257 20,000 generations.

To assess the robustness of these observations to an increase in the dimensionality of the phenotypes under selection, we increased the number of non-divergent phenotypes from one to nine for the case where the non-focal QTL mutational correlation = 0.75, but saw only a very modest increase in repeatability (fig. 5A). Finally, we investigated the case where mutations at the focal QTL affect fewer phenotypes than the non-focal QTL. In the two-phenotype model, this meant focal QTL mutations would only affect the divergent phenotype; in the five and ten-phenotype models, focal QTL mutations affected the divergent phenotype and one fewer non-divergent phenotypes than non-focal QTL. With high mutational correlation between phenotypic effects, high levels of repeatability at the focal QTL are observed, however when mutational correlations are weak or absent, very little repeatability is observed (fig. 5B).

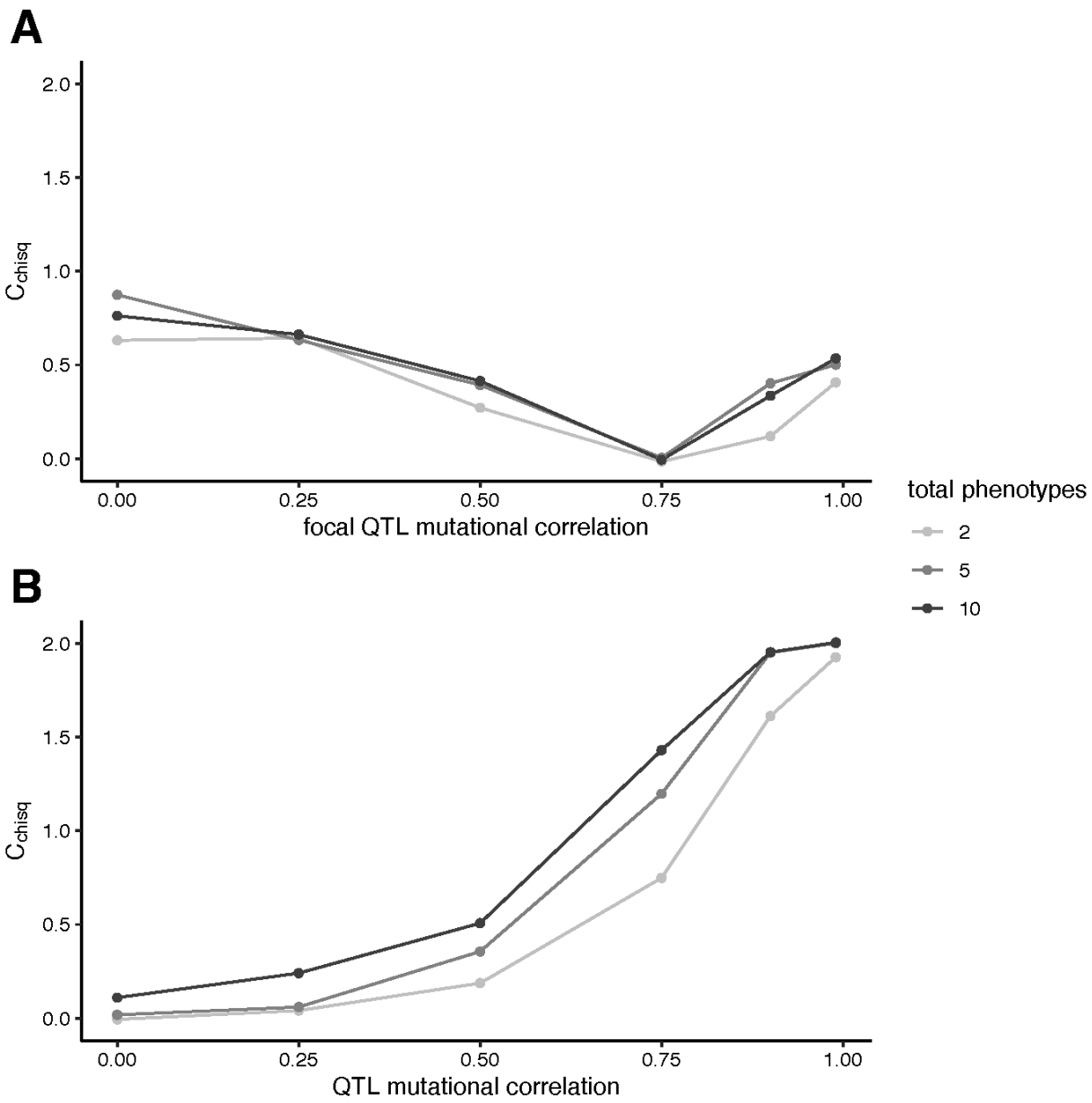

Figure 5. Repeatability (C_{chisq}) against focal QTL mutational correlation where the non-focal QTL mutational correlation = 0.75 (A) and repeatability against QTL mutational correlation where all QTL share the same mutational correlation, but the focal QTL affects the divergent phenotype (Z_1) and one fewer non-divergent phenotypes than the non-focal QTL (B). Shades indicate the total number of phenotypes in the simulation (two with one non-divergent phenotype, five with four non-divergent phenotypes and ten with nine non-divergent phenotypes). These simulations use a migration rate of 0.005 and an α^2 of 0.1, and were run for 20,000 generations.

Discussion

Empirical observations of convergent genetic evolution are common (reviewed in [5]), but in many ways at odds with some models of complex trait architecture. In this study we used simulations to understand the factors that could be varied at a QTL to produce convergent evolutionary patterns. Firstly, we demonstrated that an increase in effect magnitude (a^2) of a QTL will produce patterns of repeatability, which is consistent with previous theoretical [24] and empirical observations (e.g. [28,29]). Both mutational correlations and migration can force adaptation away from phenotypic optima along 'genetic lines of least resistance' [27,30]. Correspondingly, we see a reduction in trait divergence between demes as mutational correlation or migration is increased (fig. 2B). However, while increasing mutational correlations reduce repeatability, migration amplifies it (fig. 3A).

We also investigated how varying pleiotropy at the focal QTL affected signatures of repeatability. Pleiotropy was varied in two ways: a relaxation in mutational correlations with a non-divergent phenotype, or a reduction in the number of phenotypes that a QTL mutation affects. Congruent with the findings of Chevin, Martin & Lenormand [24] who examined single populations, we found that variation in different forms of pleiotropy will increase the likelihood that repeatability will emerge for loci governing local adaptation. Specifically, we find that a reduction in pleiotropic dimensionality at a focal QTL produces greater levels of repeatability than a relaxation in mutational correlations, a pattern that is robust to increases in trait dimensionality in our models (fig. 6A c.f. B).

Whereas Chevin, Martin & Lenormand [24] used a single phenotype in a single deme under divergent selection, our simulations used two demes linked by varying amounts of migration. This models a common situation in local adaptation: Individuals in one population may experience local environmental shifts; they must therefore adapt to new optima for some phenotypes, while retaining existing optima at others. Previously, Yeaman & Whitlock [22] demonstrated that migration concentrates the genetic architecture of local adaptation and favors alleles of larger effect. Correspondingly, we find that migration increases the observed repeatability arising from effect-magnitude variation (fig. 3, fig. S1), as high migration rates favour adaptation by larger effect alleles, which can most readily occur at the focal QTL when pleiotropy is present. But this effect breaks down as migration increases further, at which point swamping tends to prevent persistent divergence. We also find that migration increases repeatability arising from pleiotropic variation (fig. S3). This is because repeatability is driven by

the net effect of selection on a QTL. Under migration-selection balance those QTL with larger net beneficial effects (weaker mutational correlations) will be maintained as differentiated (unless migration is so high that no mutations meet the threshold).

Guillaume [27] utilized a similar two-patch design to investigate the effects of pleiotropy and migration on population divergence of phenotypes. He demonstrated that combinations of migration and pleiotropy can drive divergence between demes at phenotypes that share the same optima in both demes, as long as the phenotypes are sufficiently correlated with divergently selected phenotypes. We observe similar patterns in our simulations: Increasing levels of mutational correlations and migration reduce differentiation between demes at the divergent phenotype, and increase differentiation between demes in phenotypes not under divergent selection (fig. S3). Perhaps surprisingly, we show that this reduced phenotypic differentiation does not necessarily limit genetic repeatability, as high C_{chisq} values are observed in simulations where pleiotropy and migration have substantially limited the divergence between demes (fig. 2; 3).

Our simulations provide important insights for studies of local adaptation. Firstly, in the presence of adequate levels of migration, repeatability is expected to occur across lineages undergoing local adaptation to similar optima, even if strong pleiotropic relationships oppose the direction of divergence in phenotypic space (fig. 3). Secondly, repeated use of a QTL down multiple lineages may arise because the QTL has a disproportionately large effect size (fig. 3), but also because pleiotropy at the QTL (either the amount of correlation between traits or the number of traits affected) is relaxed (fig. 4; 5). Finally, for mutational correlations between divergent and non-divergent traits to influence repeatability, the correlations must be high, so that fortuitous pleiotropy-breaking mutations are substantially limited (fig. S2).

However, our simulations make a number of assumptions that are almost certainly violated in natural populations exhibiting evolutionary convergence. Firstly, we treat each simulation replicate as if it were a different species representing an independent bout of adaptation, and we assume complete orthology between QTL in replicates and that orthologous QTL retain corresponding effect magnitude and pleiotropic properties. In nature, divergence between species limits studies of convergence to the orthologous portions of their genomes and the effects of adaptation in non-orthologous regions has not been addressed here. Secondly, we have simulated both the initial phenotypic optima (to which both demes start our simulations

344 adapted) and the divergent phenotypic optima as identical between replicates. Populations
345 adapting to similar environments will not share identical phenotypic optima, which is important
346 for the interpretation of our results, as Thompson, Osmond & Schluter [31] observed that
347 repeatability declines rapidly as the angle between phenotypic optima increases, a pattern that
348 is exacerbated by increased trait dimensionality. Furthermore variation between QTL in
349 mutation rate, retention of standing variation and patterns of linkage disequilibrium may all affect
350 the likelihood of repeatability, but we have held these parameters constant in our simulations.
351
352 The simulations presented here also use a simplified genome architecture: four QTL with
353 uniform properties and a single QTL with aberrant properties, and between two and ten traits.
354 This system pales in comparison to the thousands of genes (exhibiting near-global pleiotropy)
355 which contribute to traits under the omnigenic model [8,13]. Contrastingly, a metaanalysis of
356 gene knockout experiments in *Saccharomyces cerevisiae*, *Caenorhabditis elegans* and *Mus*
357 *musculus* [32] estimated pleiotropy to be far less pervasive: a median gene affects only one to
358 nine percent of traits. Wang, Liao & Zhang [32] also detected significant signals of modular
359 pleiotropy (where subsets of genes affect subsets of traits), which would serve to simplify the
360 architecture available for evolutionary convergence. Simple genetic architecture enhances
361 repeatability at a genome-wide level, and this study suggests that an even more modular
362 architecture at some QTL will act to further magnify repeatability. While the nature of pleiotropic,
363 quantitative traits in higher organisms remains unresolved, we expect our simple model to be
364 applicable to more complex architectures [6], and repeating our simulations on models with 20
365 QTL yields comparable results (fig. S4).

Supplementary figures

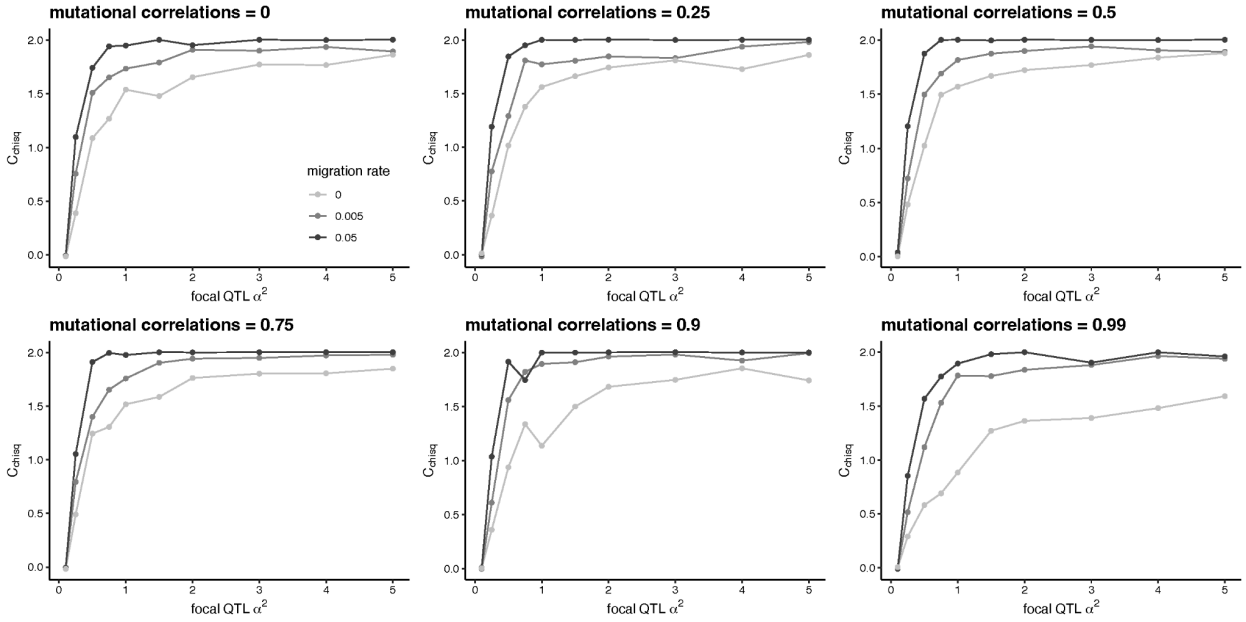

Figure S1. Repeatability (C_{chisq}) in Z_1 against focal QTL a^2 where the a^2 for non-focal QTL is 0.1. These simulations use two phenotypes (one divergent and one non-divergent), and were run for 20,000 generations.

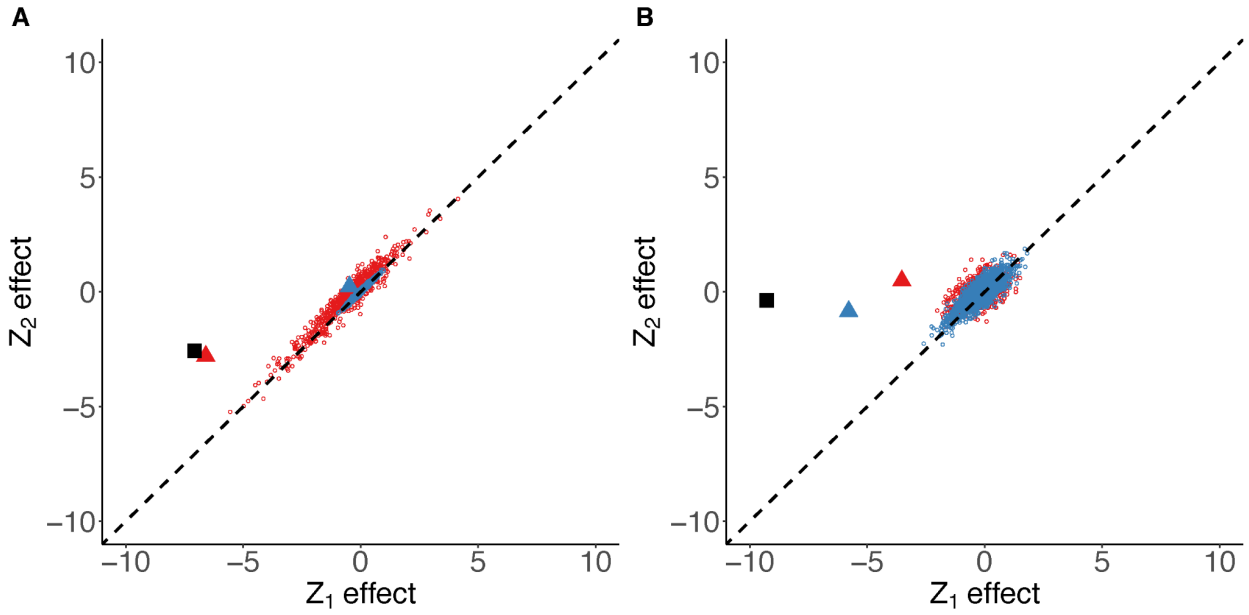

Figure S2. Phenotypic effects for all mutations occurring in d_2 across 100 replicates for single combinations of parameters (A: two phenotypes; five QTL; focal QTL $\alpha^2 = 5$; non-focal QTL $\alpha^2 = 0.1$; mutational correlations = 0.99; migration rate = 0.005; B: two phenotypes; five QTL; $\alpha^2 = 0.5$; focal QTL mutational correlations = 0.75; non-focal QTL mutational correlations = 0.9; migration rate = 0.005). Red points represent mutations at the focal QTL; blue points represent mutations at non-focal QTL. The mean divergence across replicates for focal and non-focal QTL is represented by red and blue triangles respectively, and the mean overall divergence by the black square.

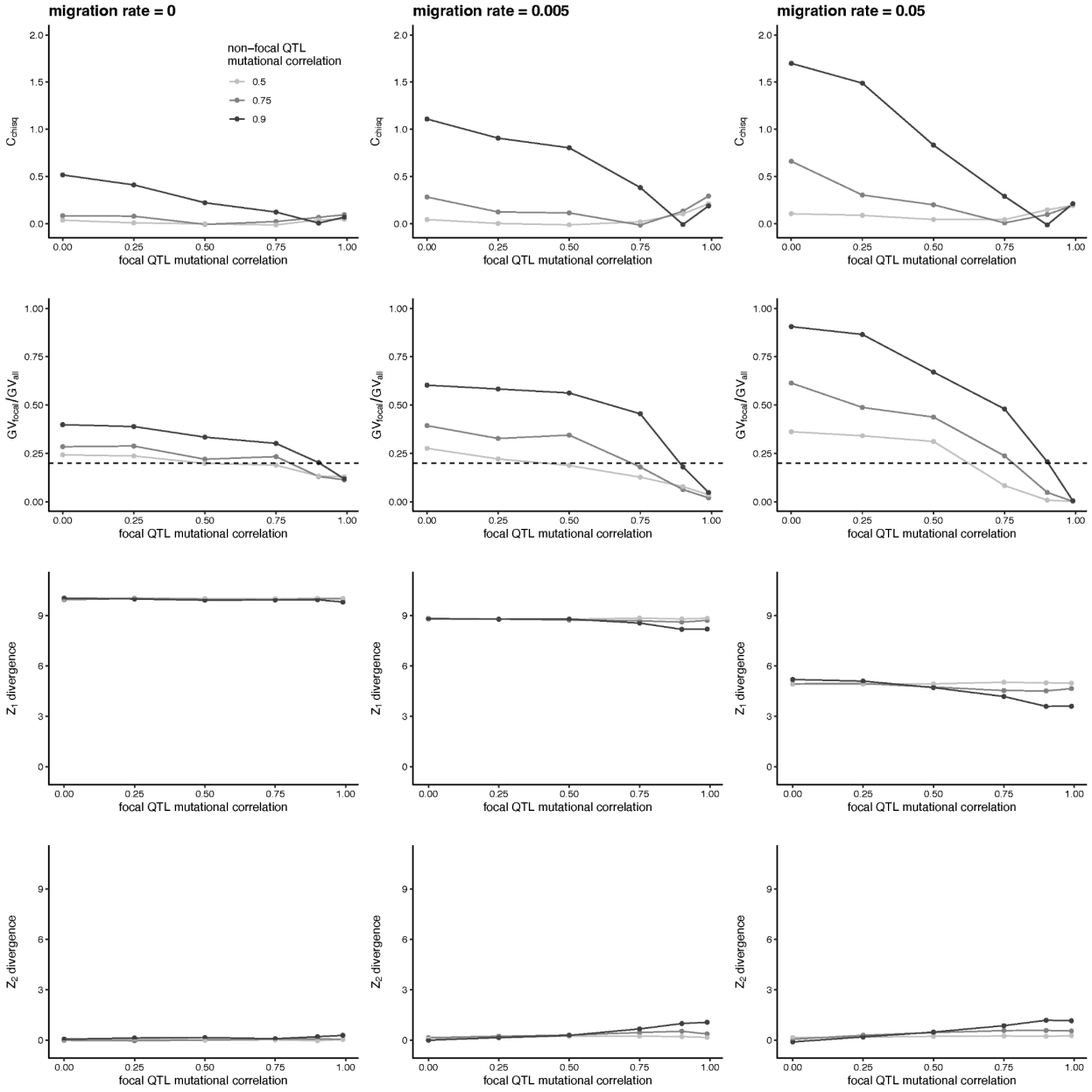

Figure S3. Repeatability (C_{chisq}) in Z_1 against focal QTL mutational correlation for varying values of non-focal QTL mutation correlation (top row), the mean proportion of all *GV* explained by *GV* at the focal QTL (second row), and divergence between demes in Z_1 (third row) and Z_2 (bottom row). These simulations use an a^2 of 0.5 and two phenotypes (one divergent and one non-divergent), and were run for 20,000 generations.

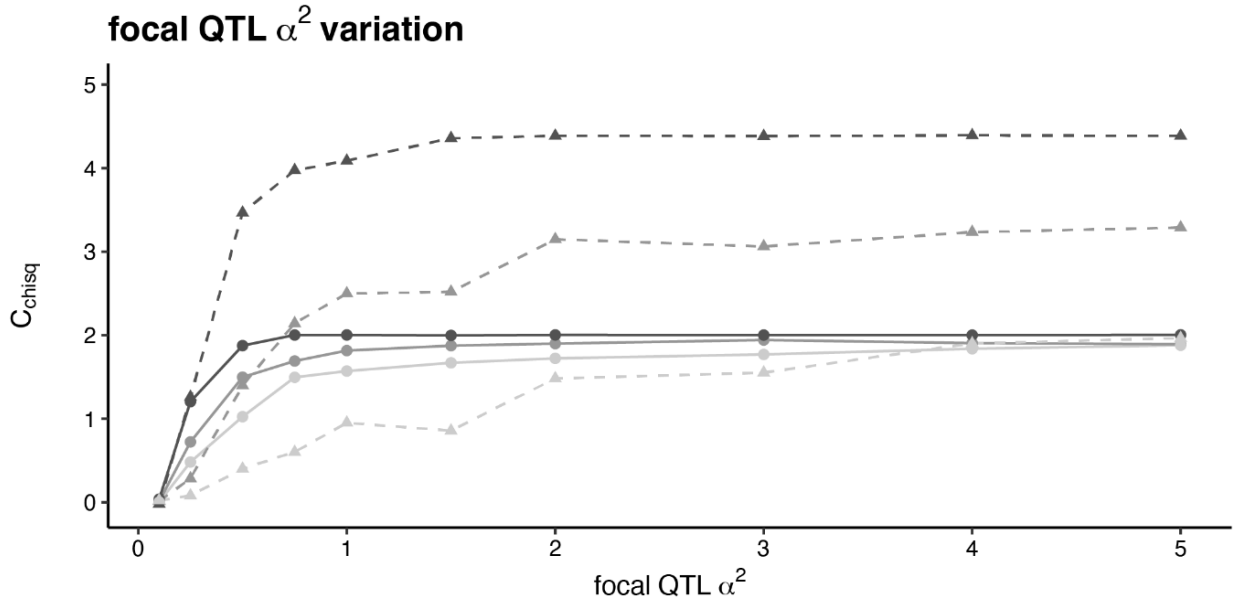

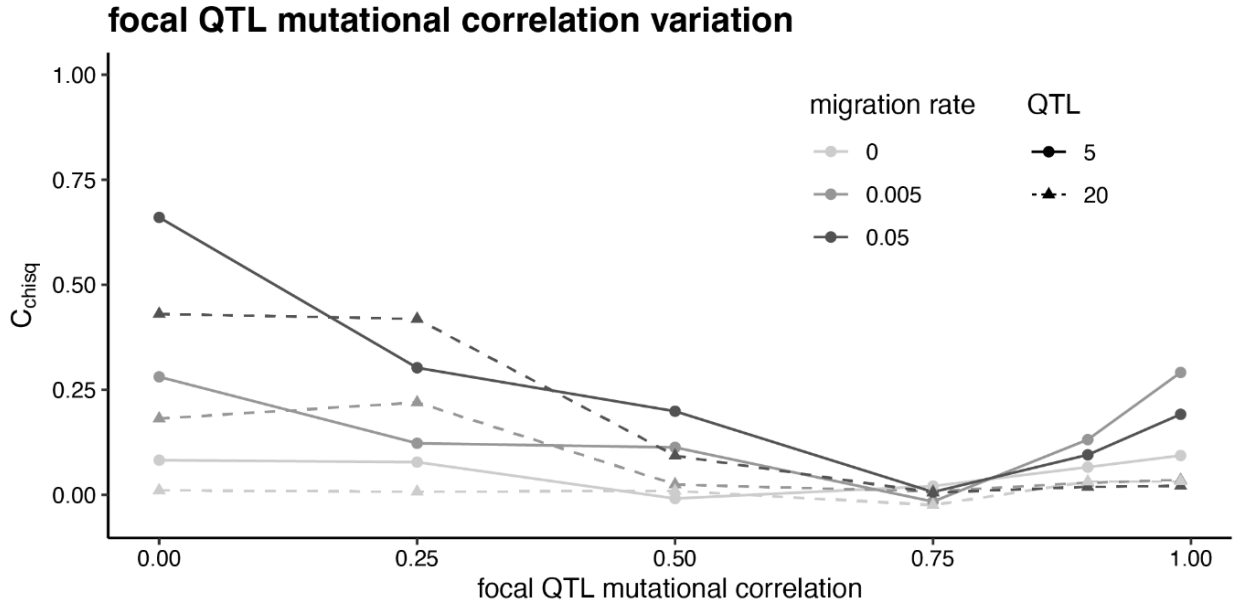

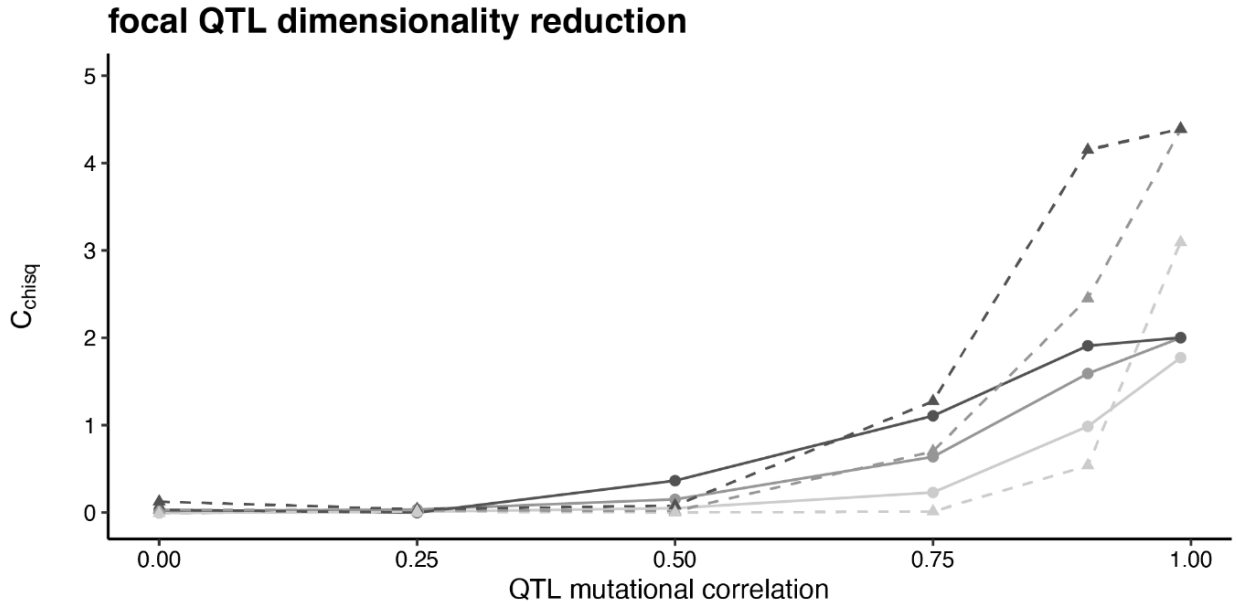

Figure S4. Effects of increasing the number of QTL modelled from five (solid lines, circle points) to 20 (dashed lines, triangle points). In the top pane we examine effect-magnitude variation at the focal QTL (as in fig. 2), with mutational correlations for all QTL fixed at 0.5. In the middle pane we examine mutational correlation variation at the focal QTL (as in fig. 4), with mutational correlations at non-focal QTL of 0.75 and α^2 at 0.5. In the lower pane we examine a reduction in dimensionality at the focal QTL (as in fig. 5B), where the total number of phenotypes is two and α^2 is 0.5.

References

1. Chan YF *et al.* 2010 Adaptive evolution of pelvic reduction in sticklebacks by recurrent deletion of a Pitx1 enhancer. *Science* **327**, 302–305.

2. Yeaman S *et al.* 2016 Convergent local adaptation to climate in distantly related conifers. *Science* **353**, 1431–1433.

3. Bohutínská M, Vlček J, Yair S, Laenen B, Konečná V, Fracassetti M, Slotte T, Kolář F. 2021 Genomic basis of parallel adaptation varies with divergence in Arabidopsis and its relatives. *Proc. Natl. Acad. Sci. U. S. A.* **118**. (doi:10.1073/pnas.2022713118)

4. Tittes S, Lorant A, McGinty S, Doebley JF, Holland JB, de Jesus Sánchez-González J, Seetharam A, Tenaillon M, Ross-Ibarra J. 2021 Not so local: the population genetics of convergent adaptation in maize and teosinte. *bioRxiv*. , 2021.09.09.459637. (doi:10.1101/2021.09.09.459637)

5. Conte GL, Arnegard ME, Peichel CL, Schluter D. 2012 The probability of genetic parallelism and convergence in natural populations. *Proc. Biol. Sci.* **279**, 5039–5047.

6. Yeaman S, Gerstein AC, Hodgins KA, Whitlock MC. 2018 Quantifying how constraints limit the diversity of viable routes to adaptation. *PLoS Genet.* **14**, e1007717.

7. Fisher RA. 1919 XV.—The Correlation between Relatives on the Supposition of Mendelian Inheritance. *Earth Environ. Sci. Trans. R. Soc. Edinb.* **52**, 399–433.

8. Boyle EA, Li YI, Pritchard JK. 2017 An Expanded View of Complex Traits: From Polygenic to Omnigenic. *Cell* **169**, 1177–1186.

9. Fisher RA. 1930 *The Genetical Theory of Natural Selection*. The Clarendon Press.

10. Visscher PM, Wray NR, Zhang Q, Sklar P, McCarthy MI, Brown MA, Yang J. 2017 10 Years of GWAS Discovery: Biology, Function, and Translation. *Am. J. Hum. Genet.* **101**, 5–22.

11. Kimura M. 1983 *The Neutral Theory of Molecular Evolution*. Cambridge University Press.

12. Orr HA. 1998 The population genetics of adaptation: The distribution of factors fixed during adaptive evolution. *Evolution* **52**, 935–949.

13. Liu X, Li YI, Pritchard JK. 2019 Trans Effects on Gene Expression Can Drive Omnigenic Inheritance. *Cell* **177**, 1022–1034.e6.

14. Orr HA. 2005 The probability of parallel evolution. *Evolution* **59**, 216–220.

15. McKenzie JA, Batterham P. 1994 The genetic, molecular and phenotypic consequences of selection for insecticide resistance. *Trends Ecol. Evol.* **9**, 166–169.

16. Shapiro MD, Marks ME, Peichel CL, Blackman BK, Nereng KS, Jónsson B, Schluter D, Kingsley DM. 2004 Genetic and developmental basis of evolutionary pelvic reduction in threespine sticklebacks. *Nature* **428**, 717–723.

17. Doebley J. 2004 The genetics of maize evolution. *Annu. Rev. Genet.* **38**, 37–59.

18. Maynard Smith J, Haigh J. 1974 The hitch-hiking effect of a favourable gene. *Genetics Research* **23**, 23–35.

19. Kaplan NL, Hudson RR, Langley CH. 1989 The 'hitchhiking effect' revisited. *Genetics* **123**, 887–899.

20. Barghi N, Schlötterer C. 2020 Distinct Patterns of Selective Sweep and Polygenic Adaptation in Evolve and Resequence Studies. *Genome Biol. Evol.* **12**, 890–904.

21. Schluter D, Marchinko KB, Arnegard ME, Zhang H, Brady SD, Jones FC, Bell MA, Kingsley DM. 2021 Fitness maps to a large-effect locus in introduced stickleback populations. *Proc. Natl. Acad. Sci. U. S. A.* **118**. (doi:10.1073/pnas.1914889118)

22. Yeaman S, Whitlock MC. 2011 The genetic architecture of adaptation under migration-selection balance. *Evolution* **65**, 1897–1911.

23. Boyle R. 1665 An account of a very odd monstrous calf. *Philosophical Transactions of the Royal Society of London* **1**, 10–10.

24. Chevin L-M, Martin G, Lenormand T. 2010 Fisher's model and the genomics of adaptation: restricted pleiotropy, heterogenous mutation, and parallel evolution. *Evolution* **64**, 3213–3231.

25. Hether TD, Hohenlohe PA. 2014 Genetic regulatory network motifs constrain adaptation through curvature in the landscape of mutational (co)variance. *Evolution* **68**, 950–964.

26. Haller BC, Messer PW. 2019 SLiM 3: Forward Genetic Simulations Beyond the Wright–Fisher Model. *Mol. Biol. Evol.* **36**, 632–637.

27. Guillaume F. 2011 Migration-induced phenotypic divergence: the migration-selection balance of correlated traits. *Evolution* **65**, 1723–1738.

28. Rosenblum EB, Hoekstra HE, Nachman MW. 2004 Adaptive reptile color variation and the evolution of the Mc1r gene. *Evolution* **58**, 1794–1808.

29. Schlenke TA, Begun DJ. 2004 Strong selective sweep associated with a transposon insertion in Drosophila simulans. *Proc. Natl. Acad. Sci. U. S. A.* **101**, 1626–1631.

30. Schluter D. 1996 ADAPTIVE RADIATION ALONG GENETIC LINES OF LEAST RESISTANCE. *Evolution* **50**, 1766–1774.

31. Thompson KA, Osmond MM, Schluter D. 2019 Parallel genetic evolution and speciation from standing variation. *Evol Lett* **3**, 129–141.

32. Wang Z, Liao B-Y, Zhang J. 2010 Genomic patterns of pleiotropy and the evolution of complexity. *Proc. Natl. Acad. Sci. U. S. A.* **107**, 18034–18039.